scientific reports

Check for updates

OPEN

# Processing of high temperature alumina/aluminum titanate ceramic composites from clean sources

Nada H. A. Besisa✉, Dina H. A. Besisa✉ & Emad M. M. Ewais

**Producing new technological materials with high performance from clean sources has become a global requirement. Alumina/aluminum titanate ($Al_2O_3/Al_2TiO_5$) composites are high-temperature portentous materials used in various advanced applications. In this work, different $Al_2O_3/Al_2TiO_5$ composites were obtained with high thermal and mechanical properties for high-temperature applications by a low-cost process. The targeted composites were produced from calcined alumina and, rutile ore extracted from the Egyptian black sands by pressureless sintering at a temperature of 1650 °C/2 h. Rutile was added to alumina with a different content (0–40 wt%) to promote its sinterability and thermo-mechanical response. Evaluation of the produced composites in terms of phase composition, densification, microstructural features, mechanical and thermal properties was investigated. The results indicated that the addition of small amounts of rutile (10 and 20 wt%) succeeded in forming a stable $Al_2O_3/Al_2TiO_5$ composite structure. However, higher content of rutile led to the formation of $Al_2TiO_5$ rich matrix composites. Moreover, highly dense composites with harmonic microstructure and enhanced mechanical strength were attained by increasing the rutile content. The composite with only 10 wt% rutile addition gave the highest density of 3.6 g/cm$^3$ and the highest cold crushing strength and modulus of rupture values of 488.73 MPa and 106.19 MPa, respectively. Notably, the addition of rutile has a substantial effect on promoting the thermal properties and thermal stability of the obtained composites up to a high temperature of 1400 °C. The present study shows that addition of rutile ore to alumina is one economical way of improving the densification and thermal expansion of $Al_2O_3$ for high temperature applications. Using a clean source such as rutile ore that contains some thermal stabilizers as $Fe_2O_3$, $Al_2O_3$, $SiO_2$, $ZrO_2$, and MgO instead of pure $TiO_2$ has played a noticeable role in improving the reaction sintering and resulting in a highly qualified material. Thus, sintered $Al_2O_3/Al_2TiO_5$ composites can be considered as a promising high-temperature material for advanced applications.**

Nowadays, with the continuous development of the different sectors of industry, the processing of high-temperature advanced materials has become an urgent requirement. It was established that high temperature materials are those withstanding temperature environments in the range of 500–600 °C[1–4]. So, ceramic and refractory materials were considered as the most promising candidates for high-temperature applications. It was also found that the suitability and sustainability of materials for high temperature applications relied on their high temperature thermal and mechanical performance as well as their production costs. Moreover, from the economic and industrial points of view, one of the most critical issues facing these high-temperature materials is decreasing their cost[5]. Thus, the main challenge is obtaining high-temperature materials with high thermal and mechanical properties with low cost.

One of the most known high-temperature ceramic materials is alumina ($Al_2O_3$, A). It is a well-known structural ceramic material that can be widely employed in various fields of applications due to its superior properties. Some of these properties are high melting point, chemical inertness, good corrosion resistance, wear resistance, hardness, high insulation, and ease of processing. However, catastrophic failure of alumina occurs in an acute thermal environment owing to large stresses sophisticated over thermal variations. Moreover, despite the high

Refractory & Ceramic Materials Division (RCMD), Central Metallurgical R&D Institute (CMRDI), P.O. Box 87, Helwan, Cairo 11421, Egypt. ✉email: nadaamin129@gmail.com; dina_hussien2002@yahoo.com

mechanical strength of alumina, its high thermal expansion ($\alpha_{20-1000\,^{\circ}C} = 8 * 10^{-6}\ K^{-1}$) and thermal conductivity, limit its range for some high-temperature structural applications[6–9].

Furthermore, aluminum titanate ($Al_2TiO_5$, AT) is a promised high-temperature ceramic material characterized by outstanding thermal shock resistance, high corrosion resistance, and low coefficient of thermal expansion. Hence, it has been considered as a successful candidate in various severe thermal environments, such as thermal processing technology, thermal insulation, refractory, metallurgy, glass and automotive industry, and engine components[8–15].

Also, AT was used as a ceramic additive to improve the thermal and mechanical properties of some ceramic composites[16]. In addition, some studies have confirmed that the insertion of AT into alumina ceramics enhances their fracture toughness and mechanical properties. This enhancement has resulted from the local residual stresses induced by the large mismatch in the thermal expansion coefficient between A and AT[16–19]. It was also found that the addition of $Al_2TiO_5$ to $Al_2O_3$ composites led to the formation of a new material with better flaw-tolerance properties[17,18].

Accordingly, combining A and AT into one composite structure will play a vital role in enhancing the thermo-mechanical response of alumina and overcome the noteworthy issues of AT ceramics[20,21], giving a new tailored material with enhanced characteristics for advanced high-temperature applications. The functional and structural properties of the tailored A/AT ceramics have made them suitable for a vast range of advanced applications, such as exhaust filter components for diesel engines, high-temperature ceramic substrates, thermocouple sheaths, in addition to thermal barrier coating and other applications[6,8,9].

Limited studies have investigated the preparation and characterization of A/AT ceramic systems[6,8–11,16–19]. In these previous works, A/AT ceramics were obtained by either the solid-state reaction between A and titanium dioxide ($TiO_2$, T) or the direct sintering of A and AT[6,22]. However, the production cost of pure T is relatively high and is a complicated process. To the best of our knowledge, no work has obtained A/AT structures from clean natural sources.

Furthermore, different methods for producing high temperature ceramic materials were reported such as hot pressing, spark plasma sintering, chemical vapor deposition, sol–gel processing, self propagating combustion synthesis and others[16–19]. However, these techniques require complicated processing and highly expensive starting materials. In contrast, pressureless sintering is a very simple and cost effective method. It is the simplest method of shaping material powders and not demands any external force other than the constraints of the mould wall, gravity and atmospheric pressure. It can be provided for sintering of refractory materials as well as oxide ceramics or carbide and nitride materials. So that, from the industrial estimation pressureless sintering method is the most appropriate method to prepare advanced materials with high efficiency and low cost[10,11].

On the other side, rutile is the most widespread mineral, composed mainly of titanium dioxide. Its refractive index is considered one of the highest indices of all known minerals. It has been used in the manufacturing of refractory and ceramic materials and various industrial applications. It was found that the best economical method for rutile extraction is by recuperating it from weathered deposits in mineral sands[23,24].

Furthermore, the Egyptian black sands contain several economic minerals. Rutile is considered one of the exceedingly significant minerals in these black sands. Most of the individual economic minerals from the Egyptian black sands, including rutile, can be obtained with marketable grades and accepted recoveries by using different low-cost and simple techniques, such as wet-gravity concentration, and magnetic separation techniques[25]. So, rutile ore extracted from black sand minerals is strongly approved to be the main source of titanium dioxide ceramics.

Once the titanium containing ores (e.g. rutile), have been mined, they have to be covered into pure titanium oxide. One of the main production methods of TiO2 is the chloride process, in which rutile can be used. This process requires large amounts of critical chemicals and remarkable quantities of energy. Apart from waste (solid or liquid) of unreacted minerals or different chlorine compounds, the chloride operation can output gaseous particulates, chlorine and sulfur dioxide emissions[23]. According to variety of problems result from the manufacture of pure titanium dioxide involving high energy cost, consumption of hazardous chemicals, production of plenty amounts of hazardous gases, acidic emissions along with wastes, which could cause considerable harm to the environment. Rutile ore is strongly suggested to be directly used in several industries[24,25]. So that the main target of this work is synthesis of high temperature industrial ceramic materials with optimized thermal and mechanical properties with low cost and environmental friendly method. Consequently, for the first time, advanced high-temperature A/AT ceramic composites were produced from natural clean sources with low-cost processing. Various $Al_2O_3/Al_2TiO_5$ composites have been developed with high thermal and mechanical performance for high temperature and advanced applications. The proposed composites were produced from the solid solution reaction of calcined alumina and rutile ore extracted from the Egyptian black at a temperature of 1650 °C/2 h. Rutile was added to alumina with a different content (0–40 wt%) to promote its sinterability and thermo-mechanical response. Besides, using a clean natural source such as rutile ore which already contains some stabilizers as $Fe_2O_3$, $Al_2O_3$, $SiO_2$, $ZrO_2$, and MgO has played a significant rule in lowering the cost of the preparation process and also in modification of the prepared composites properties. Evaluation of the produced composites in terms of phase composition, densification, microstructural features, mechanical and thermal properties was evaluated and analyzed.

## Experimental procedure

**Materials and processing.** In this study, we have considered the preparation of A/AT composites from the solid-state reaction between aluminum and titanium oxides sources. The starting materials used in this work are highly pure (99.4%) calcined alumina with a main particle size of $d_{50} = 9.227$ μm. It was supplied by SALOX®M-1FG (GKE-MF), Silkem, d.o.o, Tovarniska cesta, Slovenia, Europe. Rutile ore with a main particle

| Oxide/element | $Al_2O_3$ | $TiO_2$ | $SiO_2$ | $Fe_2O_3$ | MgO | $ZrO_2$ | CaO | $Na_2O$ |
|---|---|---|---|---|---|---|---|---|
| Alumina | 99.4 | – | 0.07 | 0.02 | – | – | 0.03 | 0.48 |
| Rutile | 4.03 | 77.95 | 3.45 | 8.24 | 0.39 | 3.36 | – | 0.25 |

**Table 1.** Chemical composition, wt% of the starting materials.

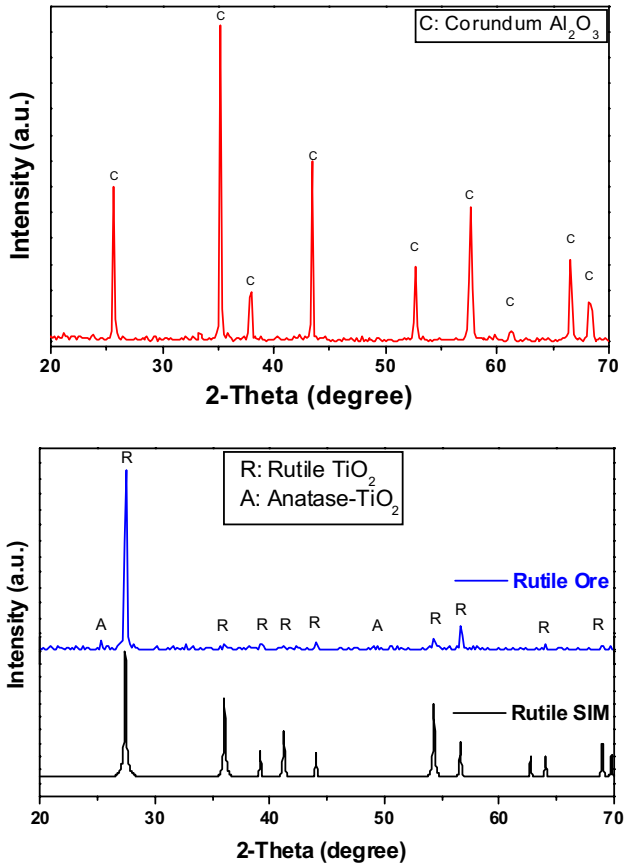


**Figure 1.** XRD patterns of the starting materials: calcined alumina (**a**) and rutile ore (**b**).

| Sample | Alumina (wt%) | Rutile (wt%) |
|---|---|---|
| 0R | 100 | 0 |
| 10R | 90 | 10 |
| 20R | 80 | 20 |
| 30R | 70 | 30 |
| 40R | 60 | 40 |

**Table 2.** Designation (wt%) of the different A/AT ceramic composites.

size of $d_{50} = 2.384$ µm, from the beneficiated deposits of the black sands of the north shores, Nuclear Materials Authority of Egypt was used as the source of $TiO_2$.

Details of the starting ceramic materials in terms of chemical analysis and phase composition are illustrated in Table 1 and Fig. 1.

Five different ceramic batches of A/AT composites with various rutile ore content (0–40 wt%) were produced by powder metallurgy technology. Samples designation/nomenclature with different percentages of the starting materials of alumina and rutile is illustrated in Table 2. Each composite mixture was homogeneously mixed in ethanol through a planetary ball milling for 2 h. The mixtures were dried and sieved through < 300 µm sieve. Green compacts in cylindrical form with a diameter of 2.5 cm were produced by uniaxial pressing (KPD-30 A, Spain) at 95 MPa. The final composites were produced by pressureless sintering at a temperature of 1650 °C/2 h

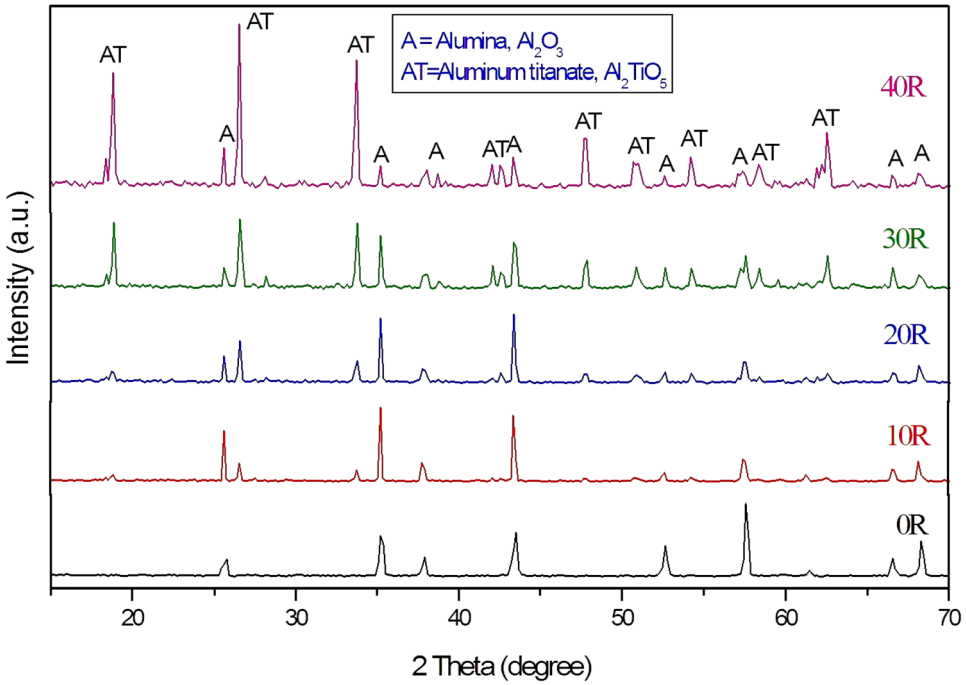


**Figure 2.** XRD pattern of the sintered A/AT composites with different rutile content (0–40 wt%).

using an electric furnace (HT 16/17, Nabertherm, Germany). The heating rate of the sintering process was kept constant at 5 °C/min.

**Characterization.** Phase analysis of the starting and different sintered composites was performed by a Brucker D8-advance X-ray powder diffractometer with Cu Ka radiation (k = 1.5406 Å). The x-ray diffractometer was attached with semi-quantitative measurements to follow up the reaction and phase content in each composite. Panalytical XRF (Model advanced axios, Netherlands) is used to determine the chemical composition of the starting materials.

Densification parameters in terms of bulk density and apparent porosity of the sintered composites were obtained by Archimedes immersion method using ethanol as an aqueous medium, ASTM C 373-72, 1984[26]. Linear shrinkage of the different composites was calculated by determining the diameter of the specimens before and after sintering.

Microstructure properties of the sintered composites were investigated by backscattered electron (BSE) in the field emission scanning electron microscopy (FESEM; QUANTA FEG250, Holland) equipped with an energy dispersive X-ray microanalyzer (EDX).

Linear thermal expansion (LTE) and its coefficient (CTE) were performed by using dilatometry (Linseis Inc., Germany, Model L76/1550) in the temperature range of room temperature up to 1400◦C with a heating and cooling rate of 10 °C/min. The measurement was performed on specimens with a determined diameter of 5 mm and a length of 35 mm. The measurement was also performed on three specimens for each composition of the obtained composites and finally was taken as average values.

Bending strength (Modulus of rupture, MOR) of the specimens was estimated by the three-point bending test using (LFM-L 20 kN, Walter + Baiag, Australian).

Cold crushing strength (CCS) was measured according to ASTM C 1424-04, 2006[27] using the universal testing machine (SHIMADZU Corporation made in Japan-model UH-F1000KN- Capacity 20-1000KN). The specimen was carefully placed into two load blocks and alignment of the specimen in the load blocks was ensured. The load was slowly applied with a crosshead rate of 1 mm/min. Cold crushing strength (CCS) was calculated according to the following formula[28]:

$$CCS = W/A$$

where CCS = Cold crushing strength ($N/mm^2$), W = Fracture load (N), A = the cross-section area of the specimen ($mm^2$).

## Results and discussion

**Phase composition and densification behavior.** Figure 2 illustrates the XRD patterns of the pressureless sintered A/AT composites at 1650 °C/2 h with different rutile content (0–40 wt%). It was noticed that for composite without rutile addition (0 R), all the identified peaks corresponded to the alumina phase only. However, upon the addition of 10 wt% rutile, aluminum titanate peaks start to appear due to the solid-state reaction formed between alumina and rutile ceramics. Increasing rutile content higher than 20 and 30% led to

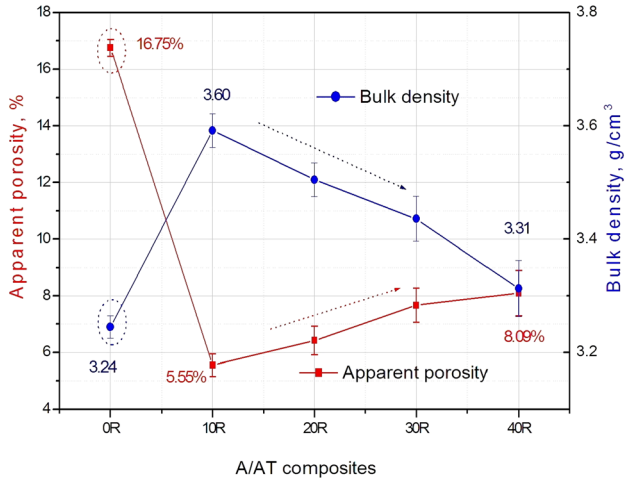


**Figure 3.** Apparent porosity and bulk density of the sintered A/AT composites with different rutile content (0–40 wt%).

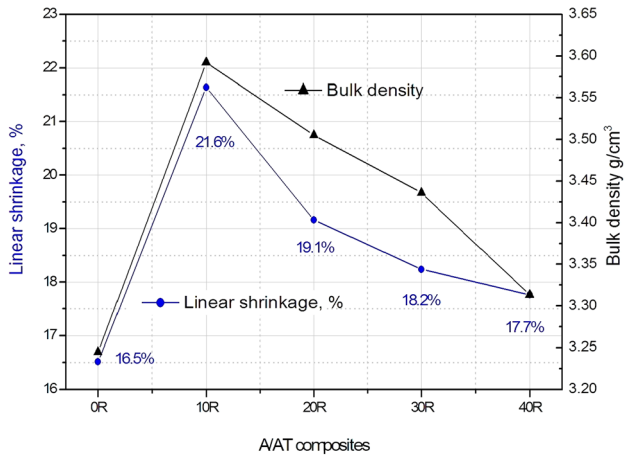


**Figure 4.** Linear shrinkage, % and bulk density of the sintered A/AT composites with different rutile content (0–40 wt%).

increasing the intensity of the formed AT peaks and decreasing alumina peaks intensity. For composite with 40% rutile addition (40 R), AT peaks become the dominant phase with a minor appearance of A peaks. So, it can be concluded that the addition of rutile with high content increases the chances of AT formation to a higher extent.

On the other hand, densification parameters in terms of apparent porosity and bulk density of the different sintered composites are measured and calculated as shown in Fig. 3. Composite 0 R without rutile addition has recorded the lowest density of 3.24 g/cm$^3$ and the highest porosity of 16.75%. However, upon the addition of 10 wt% rutile to alumina, the density of the sample enhanced and increased to 3.60 g/cm$^3$ and the porosity sharply decreased to 5.55%. This considerable enhancement of the densification parameters of A/AT composites upon the addition of small rutile content reflects its effective and positive role in alumina response. This behavior can be attributed to the homogenous diffusion of rutile in the alumina structure and the attained liquid phase reaction. In contrast, this situation is completely changed with increasing rutile content higher than 10 wt%. In another meaning, with increasing rutile content to 20%, density decreased, and porosity increased. Composite with 40% rutile gave density value of 3.31 g/cm$^3$ and porosity of about 8%. Yet, these values are still better than those achieved by the 0% rutile composite, Fig. 3. The slight reduction in the densification parameters of A/AT composites with the addition of a higher content of rutile (20–40 wt%) can be attributed to the formation of AT with higher content (as explained in XRD part, Fig. 2). It is well known that it is very difficult to attain a fully dense sintered AT structure[6,10]. Moreover, AT has a lower density than alumina[10,11]. Consequently, increasing the amount of formed AT leads to decreasing the densification of the obtained structure.

Shrinkage is a characteristic way of determining the efficiency of the sintering process. It was reported that linear shrinkage of 5–20% is a measure of highly sintered materials[29,30]. Linear shrinkage, % in diameter for the sintered A/AT composites with different rutile content (0–40 wt%) is declared in Fig. 4. Noticeably, the linear shrinkage behavior of the sintered composites is directly proportional to the bulk density. For a small amount

of rutile addition (10%), the bulk density was significantly enhanced, which resulted in increasing the the linear shrinkage. This can be explained by the grain boundary modification during the liquid phase sintering, as explained before. In contrast, the relatively small decrease in the density and linear shrinkage for higher levels of rutile may be attributed to the formed phases in each sample according to the XRD data, Fig. 2. Introducing more than 10% of rutile results in formation of more aluminium titanate, which has lower density and higher grain growth phenomena. As a conclusion, it is suggested that this reduction of linear shrinkage can be probably related to the grain growth of aluminium titanate and the formation of microcracks. The highest shrinkage rate of 21.64% is achieved by the 10 R composite, while the lowest one of 16.52% is given by the 0 R composite. This outstanding contraction rate achieved by adding only 10% rutile to alumina ceramics confirms the unique behavior of rutile addition.

**Microstructure examination.** FE-SEM micrographs with high and low magnifications of the different sintered A/AT composites are shown in Fig. 5. Microstructure of the different samples shows the intimate diffusion and distribution of the formed aluminum titanate with alumina structure that resulting from the homogenous mixing of the starting materials and the complete attained solid solution reaction. Reactivity of rutile clean source could be also taken into consideration. Concerning composite without rutile addition (0 R), alumina grains are distributed in various forms and sizes. They are distinctly present in equiaxed and cubic forms. Besides, some of them are as small as 2–5 µm. Other smaller grains are distributed in some areas of the alumina matrix. Moreover, some large grains not exceeding 10 µm are observed. The distribution of small and large grains throughout the matrix indicates a partial grain growth of alumina. The microstructure also showed some intergranular and open pores, which may be clarified by the partial grain growth of alumina. The presence of these pores results in the uncompacted structure between the grains, which explains the low density and high porosity of this sample as discussed before in the densification sections.

On the other hand, with the addition of 10 wt% rutile to alumina (10 R sample), some relatively larger grains have appeared, confirming the nucleation and formation of the AT structure. It is well known that AT grains have larger sizes than alumina ceramics. In addition, open pores have almost disappeared, and some closed pores are observed instead. The microstructure of the 10 R composite displayed reasonably dense and uniformly distributed grains in the order of 7–18 µm along with the very small grains of alumina. However, those in higher rutile added composites, such as 30 R and 40 R, seem to display a slightly greater grain size of about 10–20 µm. Moreover, some formed rounded and elongated grains are observed in these high rutile composites along with the equiaxed grains. The enhanced sintering kinetics for rutile added composites are related to the formation of a liquid phase and the second phase of AT, which fill the pores and enhance the densification[10,11,31]. Moreover, the presence of alumina with AT is expected to control the grain growth of both AT and alumina[8]. It is remarkable that with 10 wt% rutile addition, the size of alumina grains was almost like those in composite without rutile addition (0 R). In contrast, increasing rutile content higher than 20 wt% and up to 40 wt% led to abnormal grains growth of AT and finally to microcracking. This behavior can be attributed to that increasing rutile content leads to more formation of AT[6,10,11]. Consequently, the amount of existed alumina became small and not enough to completely prevent this grain growth behavior. So that, some large grains are observed in the composites with high rutile content addition (30 and 40 wt%). Also, some small microcracks are observed in the high magnification micrographs as illustrated in Fig. 6. The distribution and diffusion of alumina and AT grains (indicated with A and AT symbols) was confirmed by EDS analysis, Fig. 7.

**Mechanical properties.** Mechanical properties in terms of flexural strength (modulus of rupture: MOR) and cold crushing strength (CCS) of the sintered A/AT composites measured at room temperature are demonstrated in Fig. 8. Noticeably, the correlation between mechanical strength and rutile addition showed the same trend of the densification parameters/rutile addition curve, Fig. 3. This indicates the strong relationship between strength and density. CCS and MOR values of 226.5 MPa and 89.3 MPa respectively are obtained for the 0 R sample. With adding 10 wt % rutile, CCS and MOR values are distinguishably improved to 488.7 MPa and 106.1 MPa, respectively. Afterward, their values are gradually reduced with the continual increase of rutile content (> 10 wt%) until achieved CCS and MOR values of 219.8 MPa and 63.8 MPa, respectively for 40 R composite. Increasing the mechanical strength for composite with 10 wt% rutile may be explained by reducing the number or size of pores during the bonding of alumina and AT grains via the formed liquid phase and solid solution reaction[10,11]. While the reduction in the mechanical strength values associated with the excessive addition of rutile (20–40 wt%) may be owing to the formed phases in each batch according to the XRD data in Fig. 2. At lower levels of rutile, the main phase was $Al_2O_3$. However, insertion of more rutile, makes $Al_2TiO_5$ the major phase. In which $Al_2O_3$ is denser and has higher mechanical strength. Additionally, this behavior can be attributed to the abnormal grains growth of AT grains attached to increasing its content and the higher porosity levels of these composites. This in turn led to initiation of microcracks formation, which increases with further addition of rutile (as shown in Figs. 5 and 6) and subsequently result in lowering the mechanical strength. Moreover, it can be noticed that the mechanical strength of the obtained samples in this work is significantly greater than those reported in the literature for AT synthesized from pure oxides with further modification by various additives employing several preparation methods (see Table 3 for some comparison).

**Thermal expansion and its coefficient (LTE and CTE).** In various industrial sectors requiring fabrication and processing of high-temperature ceramic materials, many of these materials are deteriorated by the prompt changes of temperature that evolve large thermal stresses. Consequently, usability and productivity are limited. Therefore, very low thermal expansion materials are mandatory for severe thermal shock applications. Investigation of the thermal expansion behavior is very important in determining the material lifetime, suit-

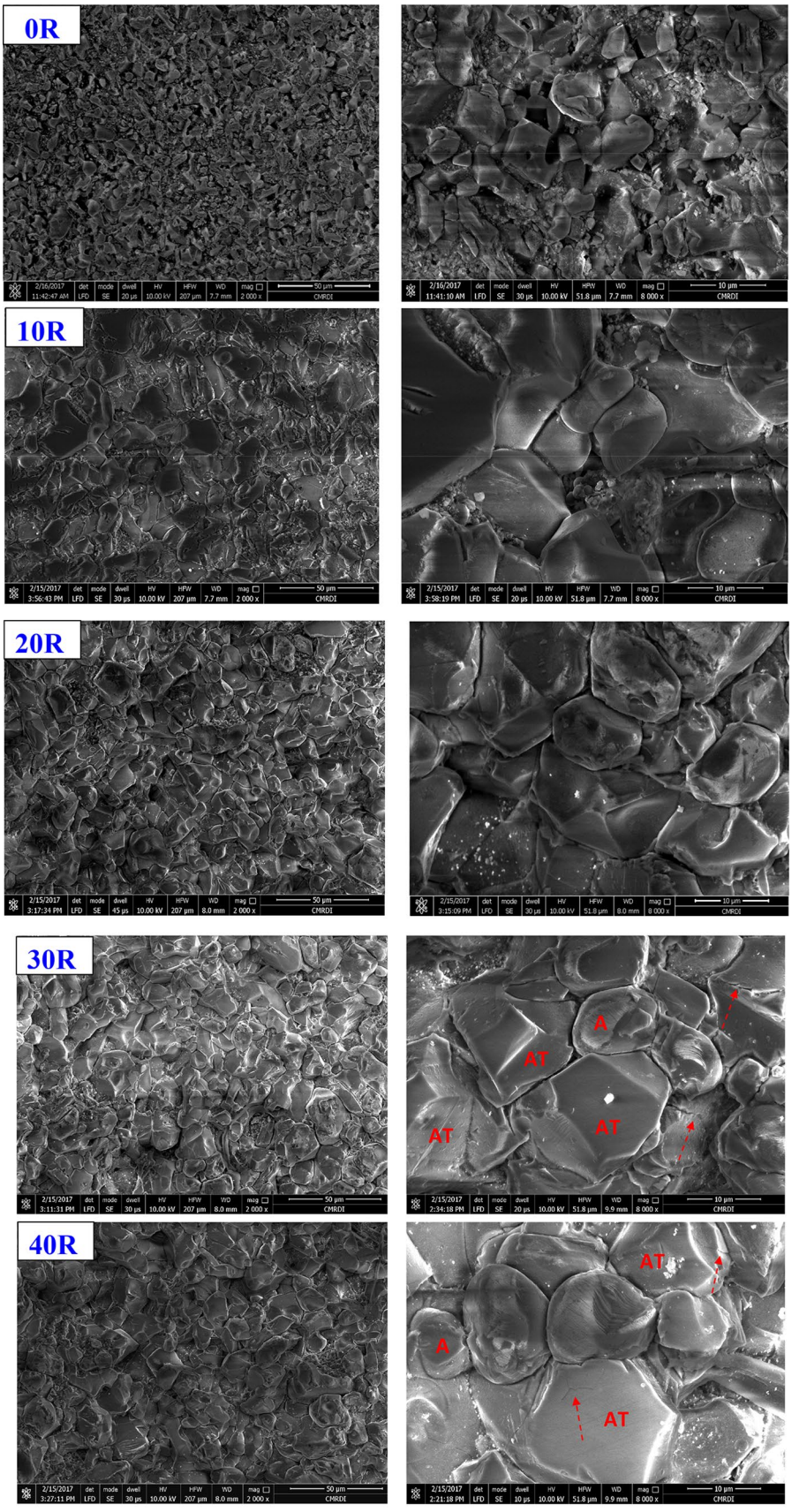


**Figure 5.** FE-SEM micrographs of the sintered A/AT composites with different rutile content (0–40 wt%).

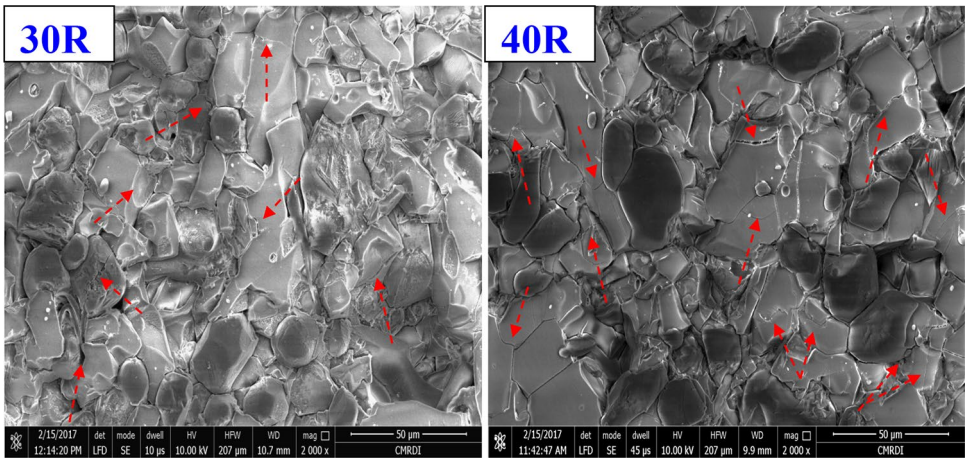


**Figure 6.** Microcracks distribution in sintered composites with high rutile content (30 and 40 wt%).

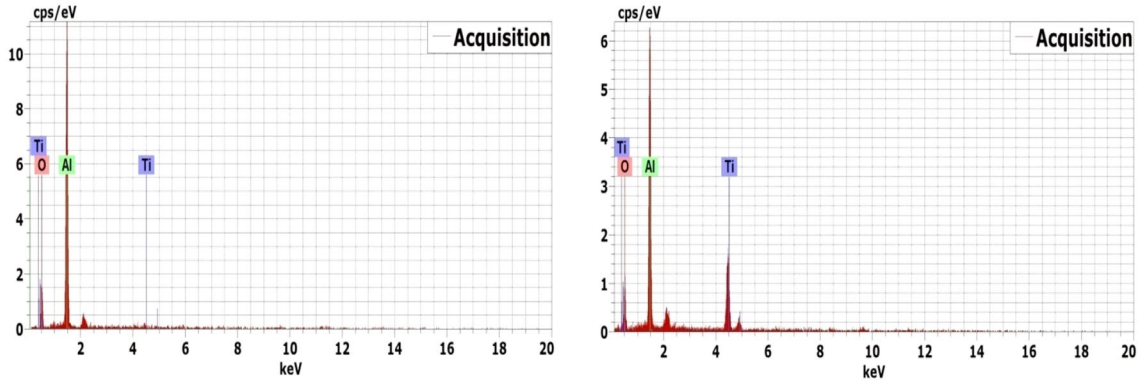


**Figure 7.** EDS analysis of alumina and aluminum titanate in the sintered 30 R and 40 R composites.

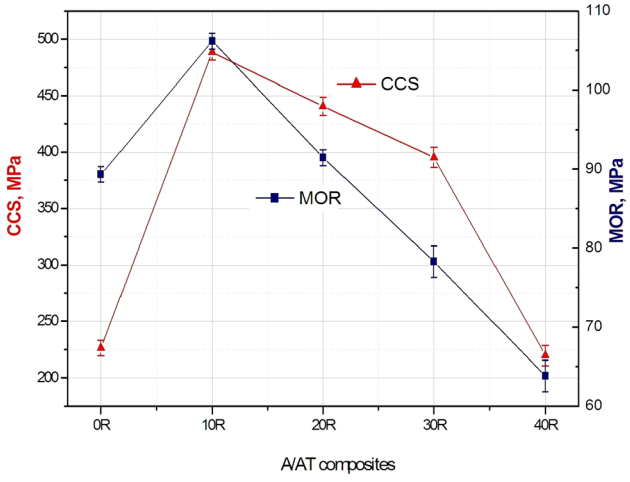


**Figure 8.** CCS and MOR of the sintered A/AT composites with different rutile content (0–40 wt%).

ability, and sustainability in high-temperature environments[29,30]. Linear thermal expansion (LTE) and its coefficient (CTE) of the sintered A/ AT composites (0–40 wt% rutile addition) as a function of temperature (from 100 to 1400 °C) are shown in Figs. 9 and 10. It was found that the thermal expansion behavior of 0 R composite shows a distinct attitude compared to the other rutile added composites. Comparison between the thermal expansion curves of rutile added and the non added composites revealed that a continuous decrease of the ther-

| Material | Flexural strength (MPa) | Coefficient of thermal expansion ($*10^{-6}$ $K^{-1}$) | References |
|---|---|---|---|
| AT | 8.53 | 1.09 | 36 |
| AT-clay | 8.61 | 0.94 | 34 |
| AT-Talc | 25.89 | 0.4 | 34 |
| AT-MgO | 38.4 | – | 13 |
| AT-Talc | 48.5 | – | 13 |
| AT-Talc-feldspar | 34.7 | – | 13 |
| AT-mullite | 37.5 | – | 13 |
| AT-$ZrTiO_4$ | 22 | – | 31 |
| AT | – | 0 | 37 |
| AT-$ZrSiO_4$ | – | 2.7 | 37 |
| AT | 30.84 | −0.927 | 10 |
| Magnesium-AT | 9.1 | −3.32 | 11 |
| AT-$Al_2O_3$ | 63.8–106.1 | −2.34 to −8.52 | Our work |

**Table 3.** Mechanical and thermal properties of AT-based ceramic composites.

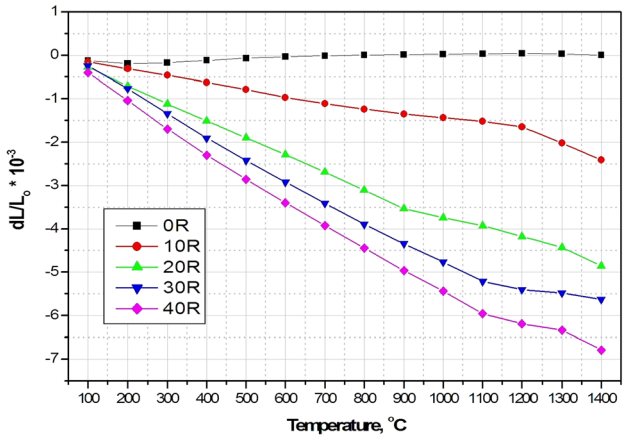


**Figure 9.** LTE of the different A/ AT composites as a function of temperature.

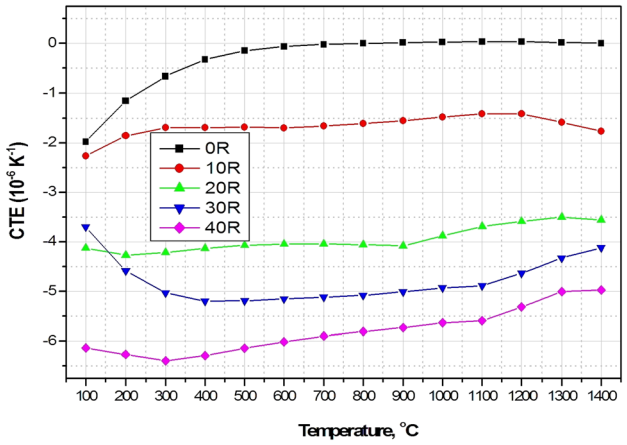


**Figure 10.** CTE of the different A/ AT composites as a function of temperature.

mal expansion value as the rutile content increases (up to 40 wt %) was detected. As can be clearly seen, with further addition of rutile, the thermal expanstion values shift towards the higher negative values. According to XRD and microstructure analysis, this behavior is believed to be due to the continuous increase of aluminium titanate besides its grain growth. Crystals of AT are made of domains with various directions. As a result, the thermal expansion ratio of AT is anisotropic. Thus, amid the cooling process, a single crystal domain of the AT

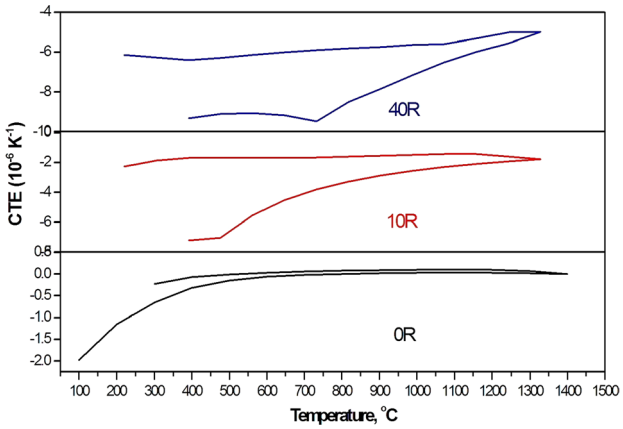


**Figure 11.** Heating/cooling curve of some selected A/ AT composites show the gradual change in the size of the formed hysteresis loop.

contracts resulting in the anisotropy and the evolution of microcracks. Otherwise, an expansion of the singular crystal domain of AT occurs amid the heating operation. Nevertheless, the expansion of the crystal domains was prohibited by the existence of microcracks[32,33]. Therefore, apparent expansion was not observed during heating of rutile added samples, which contain AT. This behavior is in good agreement with previous works[10,11,31,32,34–37]. It was found that 0 R sample gave the highest $CTE_{(100-1400\,^{\circ}C)}$ value of $0.061 * 10^{-6}\ K^{-1}$ followed by 10 R composite with a marginally lower $CTE_{(100-1400\,^{\circ}C)}$ value of $-2.34 * 10^{-6}\ K^{-1}$ and the lowest value of $-8.52 * 10^{-6}\ K^{-1}$ was recorded by 40 R composite. So that, addition of rutile to alumina was found to have a special and unparalleled role in decreasing its thermal expansion and hence enhancing its thermal performance. In addition, from Table 3 it can be seen that the coefficient of thermal expansion of our prepared AT- based composites are Cleary comparable with other AT- based materials synthesized from different starting materials and processing routes.

Moreover, cooling curves also behaved differently with all rutile added composites as shown in Fig. 11. Sintered composites exhibit a pronounced hysteresis loop, characteristic of composite materials having different thermal expansion coefficients. At higher levels of rutile addition, the hysteresis loop is quite larger, whereas the turning point of the expansion in cooling curves is continuously shifted towards the higher temperatures (from about 400 to about 700 °C) as rutile addition increases. The increased microcracks density was proved to be associated with the formation of more AT[12]. Indeed, the size of the hysteresis loop is significantly depending on the microstructure and the cracks volume. The grain size also plays an important role. The temperatures at which microcracks reopen are represented by the turning points in the cooling curves[13]. Beneath these temperatures, the amount of expansion was correlated with the density of the existing microcracks in the cooled samples. Otherwise, the expansion behavior during heating is controlled by these microcracks[13]. This can explain the small expansion starting at 400 °C on the cooling curve for the 10 R sample containing the lowest amount of AT and exhibits the lowest grain size among rutile added samples. It was also observed that this expansion increases with the increase of AT phase in the composite associated with the higher additions of rutile.

On the contrary, single-phase alumina sample (0 R) does not show such hysteresis area, Fig. 11. The absence of microcracks in this composite is the reason for this behavior[10,11]. In addition, this sample has the smallest grain size of all.

In conclusion, the addition of rutile to alumina, which resulted in the formation of AT along with alumina in the different A/AT composites, was found to be an effective way of enhancing the thermal performance of alumina. This was achieved by decreasing the thermal expansion, which in turn enhances the thermal shock resistance of the material. Moreover, the obtained composites show thermal stability without any decomposition during heating from 100 up to 1400 °C.

## Conclusions

In an attempt to develop a new high temperature and advanced material to keep up with industrial requirements, various $Al_2O_3/Al_2TiO_5$ composites were developed with high thermal and mechanical performance from a natural clean source and low cost. The proposed composites were produced from the solid solution reaction of calcined alumina and for the first time, from rutile ore extracted from the Egyptian black sand at a temperature of 1650 °C/2 h. Rutile was added to alumina with different content (0–40 wt%) to promote its sinterability and thermo-mechanical response. Highly dense composites with harmonic microstructural and enhanced mechanical strength were attained by increasing the rutile content. Composite with 10 wt% rutile gave the highest density of 3.6 g/cm$^3$ and the highest CCS and MOR values of 488.73 MPa and 106.19 MPa, respectively. Notably, the addition of rutile has a substantial effect on promoting the thermal properties and thermal stability of the obtained composites up to the high-temperature of 1400 °C. This was achieved by decreasing their thermal expansion values, which in turn enhances their thermal shock resistance. It can be concluded that using a clean natural source such as rutile ore which already contains some stabilizers as $Fe_2O_3$, $Al_2O_3$, $SiO_2$, $ZrO_2$, and MgO has played a significant rule in lowering the cost of the preparation process and also in enhancing the properties of the prepared composites. This was the main motivation behind this work, to encourage using clean sources,

instead of higher cost purified starting materials. Thus, sintered $Al_2O_3$/ $Al_2TiO_5$ composites can be considered as a promising high temperature material for advanced structural and thermal applications.

Received: 1 January 2022; Accepted: 23 March 2022
Published online: 08 April 2022

## References

1. Meetham, G. W. & Van de Voorde, M. H. Materials for high temperature engineering applications. In *Engineering Materials.* ISBN 3-540-66861-6 (Springer, 2000).
2. Gupta, O. P. *Elements of Fuels, Furnaces and Refractories* 6th edn. (Khanna Publishers, 2014).
3. Schacht, C. A. *Refractories Handbook* 1st edn. (Marcel Dekker, Inc., 2004).
4. Bengisu, M. *Engineering Ceramics* 1st edn. (Springer, 2001).
5. Blau, P. J. *Friction and Wear Transitions of Materials: Break-in, Run-in, Wear-in* 1st edn. (Noyes Publications, 1989).
6. Ananthakumar, S. & Warrier, K. G. K. Extrusion characteristics of alumina- aluminium titanate composite using boehmite as a reactive binder. *J. Eur. Ceram. Soc.* **21**, 71–78 (2001).
7. Sathiyakumar, M. & Gnanam, F. D. Influence of additives on density, microstructure and mechanical properties of alumina. *J. Mater. Process. Technol.* **133**, 282–286 (2003).
8. Yang, Y. *et al.* In situ alumina/ aluminum titanate bulk ceramic composites prepared by SPS from different structured composite powders. *J. Alloys Compd.* **481**, 858–862 (2009).
9. Mohseni, Sh., Barzegar Bafrooei, H., Ebadzadeh, T. & Tazike, M. Microstructure and mechanical properties of $Al_2O_3$-20 wt% $Al_2TiO_5$ composite prepared from alumina and titania nanopowders. *J. Ceram. Int.* **39**, 977–982 (2013).
10. Ewais, E. M. M., Besisa, N. H. A. & Ahmed, A. Aluminum titanate based ceramics from aluminum sludge waste. *J. Ceram. Int.* **43**, 10277–10287 (2017).
11. Ewais, E. M. M. & Besisa, N. H. A. Tailoring of magnesium aluminum titanate based ceramics from aluminum dross. *J. Mater. Des.* **141**, 110–119 (2018).
12. Lan, J., Yan, C. X., Ming, H. G. & Yu, M. Effect of additives on properties of aluminum titanate ceramics. *Trans. Nonferrous Met. Soc. China* **21**, 1574–1579 (2011).
13. Tsetsekou, A. A comparison study of tialite ceramics doped with various oxide materials and tialite–mullite composites: Microstructural, thermal and mechanical properties. *J. Eur. Ceram. Soc.* **25**, 335–348 (2005).
14. Huang, Y. X., Senos, A. M. R. & Baptista, J. L. Effect of excess $SiO_2$ on the reaction sintering of aluminium titanate-25 vol% mullite composites. *J. Ceram. Int.* **24**, 223–228 (1998).
15. Li, M., Chen, F., Shen, Q. & Zhang, L. Fabrication and thermal properties of $Al_2TiO_5/Al_2O_3$ composites. *J. Mater. Sci. Pol.* **28**(3), 663–670 (2010).
16. Bueno, S., Berger, M. H., Moreno, R. & Baudín, C. Fracture behaviour of microcrackfree alumina–aluminium titanate ceramics with second phase nanoparticles at alumina grain boundaries. *J. Eur. Ceram. Soc.* **28**, 1961–1971 (2008).
17. Padture, N. P., Bennison, S. J. & Chan, H. M. Flaw-tolerance and crack resistance properties of alumina–aluminium titanate composites with tailored microstructures. *J. Am. Ceram. Soc.* **76**, 2312–2320 (1993).
18. Low, I. M. Physical characteristics of an in-situ layered and graded alumina/aluminium titanate composite. *Mater. Res. Bull.* **33**, 1475–1481 (1998).
19. Baudin, C., Sayir, A. & Berger, M. H. Mechanical behaviour of directionally solidified alumina/aluminium titanate ceramics. *Acta Mater.* **54**(38), 35–41 (2006).
20. Buscaglia, V., Nanni, P., Battilana, G., Aliprandi, G. & Carry, C. Reaction sintering of aluminium titanate: I effect of MgO addition. *J. Eur. Ceram. Soc.* **13**, 411–417 (1994).
21. Perera, F. H., Pajares, A. & Meléndez, J. J. Strength of aluminiumtitanate/mullite composites containing thermal stabilizers. *J. Eur. Ceram. Soc.* **31**, 1695–1701 (2011).
22. Park, S. Y., Jung, S. W. & Chung, Y. B. The effect of starting powder on the microstructure development of alumina–aluminum titanate composites. *J. Ceram. Int.* **29**, 707–712 (2003).
23. Manufacture of titanium dioxide, learn chemistry, Enhancing learning and teaching with the RSc, WWW. Rsc.Org/ learn- chemistry maste class: $TiO_2$- sheet 5, 1–4 (The Wolfson Foundation).
24. Baba, A. F. A., Adekola, F. A., Toye, E. E. & Bale, R. B. Dissolution kinetics and leaching of rutile ore in hydrochloric acid. *J. Miner. Mater. Charact. Eng.* **8**(10), 787–801 (2009).
25. Moustafa, M. I. Mineralorgical characteristics of the separated magnetic rutile of the Egyptian black sands. *J. Sci. Minufia Univ.* **xxxIII**(2), 149–170 (2009).
26. ASTM, standard C373-72. *Test Method for Water Absorption, Bulk Density, Apparent Porosity and Apparent Specific Gravity of White Ware Products*, annual book of ASTM, vol. 15, USA (1984).
27. ASTM, standard C1424-04. *Test Method for Cold Crushing Strength of Advanced Ceramics*, annual book of standards, section 15, vol. 15, 01 (2006).
28. Zangvil, A. & Ruh, R. Phase relationships in the silicon carbide-aluminum nitride system. *J. Am. Ceram. Soc.* **71**, 884 (1988).
29. Besisa, D. H. A. & Ewais, E. M. M. Black zirconia composites with enhanced thermal, optical and mechanical performance for solar energy applications. *Sol. Energy Mater. Sol. Cells* **225**, 111063 (2021).
30. Besisa, D. H. A. *et al.* Densification and characterization of SiC-AlN composites for solar energy applications. *Renew. Energy* **129A**, 201–213 (2018).
31. Jin-Kim, I. K. & Cao, G. Low thermal expansion behavior and thermal durability of $ZrTiO_4$ $Al_2TiO_5$–$Fe_2O_3$ ceramics between 750 and 1400 °C. *J. Eur. Ceram. Soc.* **22**, 2627–2632 (2002).
32. Hong, C. & Awaji, H. Temperature dependence of mechanical properties of aluminum titanate ceramics. *J. Eur. Ceram. Soc.* **27**, 13–18 (2007).
33. Bruno, G. *et al.* Micro- and macroscopic thermal expansion of stabilized aluminum titanate. *J. Eur. Ceram. Soc.* **30**, 2555–2562 (2010).
34. Tkachenko, V. D., Garmash, E. P., Lupin, B. K. & Lugovskaya, E. S. *Thermal Expansion of Ceramics Containing Aluminum Titanate 8* 45–49 (Institute of Problems Of Materials Physics, Academy of Sciences of the Ukrainian SSR, 1988).
35. Oikonomou, P., Ch Dedeloudis, C. J. & Ftikos, S. C. Stabilized tialite–mullite composites with low thermal expansion and high strength for catalytic converters. *J. Eur. Ceram. Soc.* **27**, 3475–3482 (2007).
36. Papitha, R., Buchi Suresh, M., Das, D. & Johnson, R. Mineral-oxide-doped aluminum titanate ceramics with improved thermo-mechanical properties. *J. Ceram.* https://doi.org/10.1155/2013/214974 (2013).
37. Nagano, M., Nagashima, S., Maeda, H. & Kato, A. Sintering behavior of Al2TiO5 base ceramics and their thermal properties. *J. Ceram. Int.* **25**, 681–687 (1999).

## Author contributions

N.H.A.B.: Conceptualization, Methodology, Validation, Investigation, Writing - original draft,D.H.A.B.: Investigation, Writing - review & editing.E.M.M.E.: Conceptualization, Resources, Project administration, Supervision. All authors reviewed the manuscript.

## Funding

Open access funding provided by The Science, Technology & Innovation Funding Authority (STDF) in cooperation with The Egyptian Knowledge Bank (EKB).

## Competing interests

The authors declare no competing interests.

## Additional information

**Correspondence** and requests for materials should be addressed to N.H.A.B. or D.H.A.B.

**Reprints and permissions information** is available at www.nature.com/reprints.

**Publisher's note** Springer Nature remains neutral with regard to jurisdictional claims in published maps and institutional affiliations.